analytical chemistry

Article

Cite This: *Anal. Chem.* 2018, 90, 8960–8968

pubs.acs.org/ac

Design of Ultrasensitive Protein Biosensor Strips for Selective Detection of Aromatic Contaminants in Environmental Wastewater

Shamayeeta Ray,[†] Tamasri Senapati,[†] Subhankar Sahu,[†] Rajdip Bandyopadhyaya,[‡] and Ruchi Anand*[,†,§]

[†]Department of Chemistry, Indian Institute of Technology Bombay, Mumbai 400076, Maharashtra India

[‡]Department of Chemical Engineering, Indian Institute of Technology Bombay, Mumbai 400076, Maharashtra India

[§]Wadhwani Research Center for Bioengineering, IIT Bombay, Mumbai 400076, India

Supporting Information

ABSTRACT: Phenol and its derivatives constitute a class of highly toxic xenobiotics that pollute both river and groundwater. Here, we use a highly stable enzyme-based in vitro biosensing scaffold to develop a chip-based environmental diagnostic for in situ accurate, direct detection of phenol with selectively down to 10 ppb. Mesoporous silica nanoparticles (MCM41) having a pore diameter of 6.5 nm was screened and found to be the optimal solid support for creation of a robust immobilized protein based sensor, which retains stability, enzyme activity, sensitivity, and selectivity at par with solution format. The sensor strip exhibits minimal cross reactivity in simulated wastewater, crowded with several common pollutants. Moreover, this design is competent towards detection of phenol content with 95% accuracy in real-time environmental samples collected from local surroundings, making it a viable candidate for commercialization. The enzyme has been further modified via evolution driven mutagenesis to generate an exclusive 2,3-dimethylphenol sensor with equivalent selectivity and sensitivity as the native phenol sensor. Thus, this approach can be extended to generate a battery of sensors for other priority aromatic pollutants, highlighting the versatility of the biosensor unit. This novel biosensor design presents promising potential for direct detection and can be integrated in a device format for on-site pollutant monitoring.

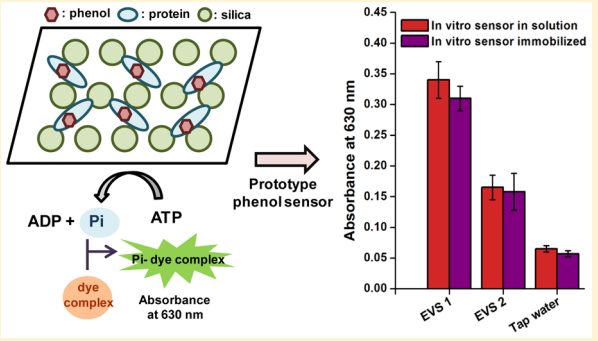

Biosensors can serve as far more specific and selective sensing units, compared to nonbiological approaches. This is mostly because the biological sensing machinery, whether it be DNA or a protein, has been perfected over eons, via evolutionary rigor.[1] Nevertheless, apart from the well established glucose oxidase based diabetes diagnostic device that has been massively successful as a worldwide portable product, there are very few examples of other biosensor devices breaking into this space.[2−4] This is mostly because of issues related to stability, selectivity, and complicated indirect signal output methods that are required for quantification of the requisite sensor element. For example, immunochemical-based protein-chips that are used in diagnostics are marred with false positives as they require a host of secondary labile reagents that induce nonspecificity leading to increased error in measurement.[5] Therefore, to ensure success, label-free biosensors coupled to instant detection technologies are the way forward.[6,7] Creation of such biosensor devices is dependent on a self-contained system that has both accurate biosensing capabilities and a coupled intrinsic readout unit, such that direct detection is made possible.

The nitrogen regulating protein C (NtrC) class of regulators present one such label-free versatile biosensing system.[8,9] NtrCs possess a modular architecture harboring a signal sensing (A) domain that allosterically represses the ATP hydrolysis of the tandemly located AAA+ ATPase (C) domain.[10,11] The basic biosensing design rests on the fact that ATP hydrolysis in NtrCs is under the tight control of the upstream sensing unit.[12,13] It is the presence of this intrinsic sensing (A) and readout system (C) in this family that makes it apt to be exploited for development of potential label free biosensor devices.[9,12] In this work, we demonstrate the proof of concept of this approach by creating a chip based in vitro biosensor of the NtrC family protein MopR from *Acinetobacter calcoaceticus* NCIB8250.[14,15] It belongs to the aromatic pollution sensor subclass and in the presence of escalated levels of the pollutants, MopR undergoes a significant allosteric conformational change that enable sensing.[14,15] Although, the native MopR enzyme is highly selective and senses only phenol and its smaller derivatives, recent studies have demonstrated that X-ray crystallography coupled with synthetic biology approaches can be employed to tweak its sensing repertoire via logic based engineering of its binding pocket.[16] This enables

Received: March 13, 2018
Accepted: July 13, 2018
Published: July 13, 2018

DOI: 10.1021/acs.analchem.8b01130
Anal. Chem. 2018, 90, 8960–8968

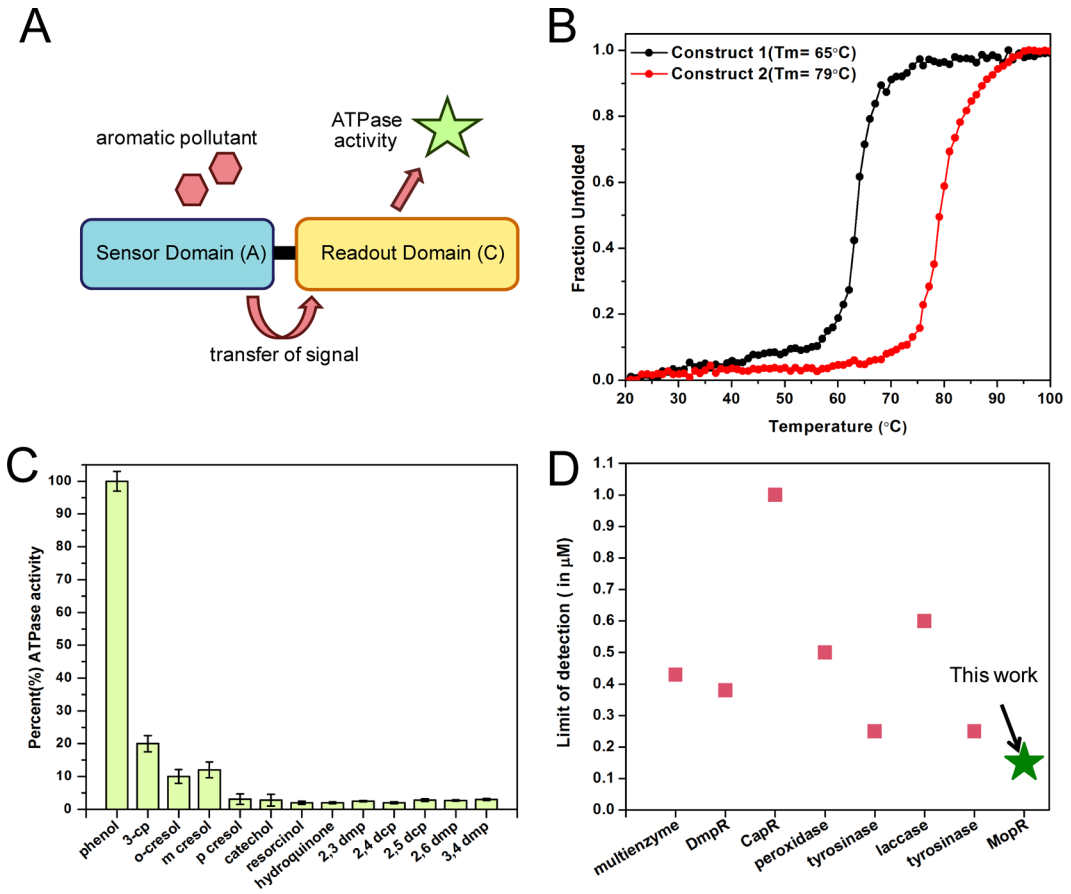

Figure 1. Optimization of in vitro biosensor design. (A) Model design of in vitro biosensor ($MopR^{ABC}$). (B) CD-based melt curve of different constructs of $MopR^{ABC}$ protein showing higher thermostability of construct 2 (T_m of 79 °C). (C) In vitro ATPase biosensing assay depicting the aromatic substrate profile of $MopR^{ABC}$, with the protein exhibiting best activity toward phenol and is nonresponsive to bulkier phenol derivatives. (D) Comparison of the limit of detection (LOD) of $MopR^{ABC}$ design with other phenol biosensors. For each biosensor type, the best LOD has been considered in the plot (refer to Table S1).

potential detection of a range of priority pollutants making MopR a generalized platform for development of environmental pollution sensors for toxic aromatic xenobiotics.

Development of environmental diagnostics for aromatic pollutant sensing has remained a daunting task. This is mostly because these compounds lack active functional groups, a perquisite for development of direct detection protocols. In absence of the above mention approach the most common detection techniques currently in use are GC-MS (gas chromatography−mass spectrometry) and LC-MS (liquid chromatography−mass spectrometry).[17] However, these methods require pretreatment processing, which make them cumbersome, expensive and time-intensive procedures.[18,19] Furthermore, GC-MS and LC-MS systems, because of their complicated detection technology, are not very portable and have limited scope for in situ direct detection with ease.[19] Hence, over the past couple of years, there has been surge in development of alternative enzyme based sensors, especially for phenol sensing.[19] For example, a combination of laccase, peroxidase, tyrosinase sensor system has been focus of development in this arena.[20−22] Unfortunately, none of these enzymes specifically sense only phenols and exhibit a poor selectivity and sensitivity profile. Moreover, since the most effective biosensor design in the laccase/tyrosinase class is a three-component enzyme system, ensuring stability of all components is convoluted, making this system complex and tough to commercialize.[19] To increase the robustness of the above systems, several efforts to enhance the overall stability have been undertaken; however, the multicomponent nature of these biosensors poses limitations in this regard.[19] As an alternative, in this work, we demonstrate that native MopR, a highly thermostable single component and selective enzyme system, is capable of surpassing the current approaches and can be successfully translated into an in vitro immobilized chip based detection format.[15] The robustness and sensitivity of the sensor chip was assessed both in water ridden with a plethora of contaminants and in real time environmental samples collected from multiple contaminated water samples in the local region. Moreover, the MopR biosensor has been intelligently tweaked by evolution guided design to sense non-native effectors like 2,3-dimethylphenol (2,3-dmp) with parts per billion level sensitivity. Thus, this system provides a platform for universal biosensor design for a spectrum of toxic pollutants and exhibits desired qualities for creation of a commercial platform for in situ aromatic pollutant monitoring.

RESULTS AND DISCUSSION

Optimization of the In Vitro Biosensor Design. For efficient design of the protein sensor strip, we first validated and fine-tuned the in vitro biosensor design.[16] As the primary sensor scaffold, the design uses the recombinant version of MopR protein, consisting of the sensor (A) and readout

DOI: 10.1021/acs.analchem.8b01130
Anal. Chem. 2018, 90, 8960−8968

ATPase domain (C) ($MopR^{ABC}$). In this design, upon binding of phenol, the ATP hydrolysis activity is induced, which is measured by a malachite green-based optical sensing method[23] (Figure 1A). The amount of ATP hydrolyzed is directly proportional to the pollutant concentration present in the test sample. On the basis of this assay, the optimal characteristics for feasibility of the biosensor were ascertained. The first task undertaken was to enhance the thermal stability of the existing design. After screening through various sensor combinations of $MopR^{ABC}$ (detailed in Supporting Materials and Methods), construct 2, possessing a T_m of 79 °C, was chosen as the template for further optimization (Figure 1B). This truncated version of $MopR^{ABC}$ protein exhibited enhanced stability and biosensor activity for a prolonged time-period at elevated temperatures, thereby making it a robust sensor system (Figure S1). Because of this superior thermal stability and single component sensing, $MopR^{ABC}$ poses to be a better biosensor candidate than other phenol sensing enzymes like tyrosinase ($T_m \approx 46$ °C) and laccase ($T_m \approx 50-60$ °C).[24,25]

Important criteria for viable biosensors, selectivity and high sensitivity, were also explored for the $MopR^{ABC}$ system. Existing phenol sensors like tyrosinases and laccase are marred with both selectivity and sensitivity issues. For instance, tyrosinases accept both mono- and di-substituted phenols, as well as amino acid substrates, like dihydroxy-phenylalanine, etc., and the laccase family display an even broader substrate profile.[26,27] This renders both these systems apt for determination of overall phenolic content in food and dye industry; however, restricting accurate, sensitive, and selective detection of a single pollutant.[27] On the contrary, the MopR transcription regulator has evolved to specifically sense phenol and trigger its catabolism. Consequently, the $MopR^{ABC}$ biosensor is suitable for very specific and highly sensitive detection of phenol, especially at lower pollutant levels (Figures 1C and S2A–D). Further, $MopR^{ABC}$ is completely nonresponsive towards any of the bulkier phenols like xylenols or dichlorophenols, even when they are present in high concentrations (Figure S2D).

To gauge the sensitivity parameters for $MopR^{ABC}$ in the current assay system, the ATP concentration was optimized and 1 mM ATP was found to be most suitable for enhanced sensitivity. Under these conditions, subtle differences of 0.1–0.2 μM pollutant concentration could be detected accurately (Figure S2E). Further, the LOD was determined to be 0.1 μM (~10 ppb), which is the best value reported until date for any enzyme-based selective phenol sensor (Figure 1D and Table S1). Hence, MopR armed with the arsenal of selectivity, sensitivity and thermal stability poses to be a very attractive and viable solution for direct phenol estimation in the low concentration regime in an environmental wastewater setting. The $MopR^{ABC}$ sensor unit harbors both the sensing (A) and ATP readout (C) domain in the same polypeptide, making signal detection reliable (Figure 1A). Moreover, under these sensitivity limits, this system can be employed for direct in situ testing of bottled water (permissible limit 5–10 ppb). A cumbersome combination of preconcentration steps with extraction of organic phenol, followed by LC-MS, currently in use by industries, can be replaced by the $MopR^{ABC}$-based direct detection system.

The main shortcoming of the $MopR^{ABC}$ sensor appears to be that, although it is highly selective and sensitive for phenol, it is unable to sense a wide range of aromatic pollutants present in wastewaters. To overcome this insufficiency and demonstrate the versatile and tunable nature of MopR, in previous reports, structure-guided design have been employed[16] (Figure S2A). Tweaking of the pocket architecture enabled engineering of a battery of recombinant protein-based sensors that encompassed a broad range of aromatic pollutants. Following this approach, selectivity was maintained; however, sensitivity below parts per million range was compromised. To overcome this deficit, evolutionary analysis by constructing sequence similarity networks of similar AAA+-containing ATPase family proteins was undertaken[28] (Figure 2A). Results reveal that several naturally occurring proteins in the aromatic pollutant sensing subclass fall in the same group (group 1, Figure 2A). Evolutionary cues were taken to efficiently tweak the selectivity profile from the created network, concerted mutations of the entire sensor pocket were considered as a viable option. Instead of constructing sensor by employing the natural proteins, this approach was necessary because most of the parent proteins are insoluble and difficult to purify in their native form. The objective was to start with the native MopR sensor, employ evolutionary design and tweak the binding pocket such that it is converted into a sensor that can accurately sense a phenol derivative but no longer senses the parent compound with high sensitivity. To demonstrate proof of concept, the dimethyl phenol sensor (DmpR) was created as a model system (Figure 2B–C). The $MopR^{FM\_IV\_YF}$ protein with identical pocket residues to DmpR protein was constructed and purified. The results showed that the evolution based design was very successful and the $MopR^{FM\_IV\_YF}$ exhibits exclusive and highly sensitive response to the bulky phenol, 2,3-dmp, in the low ppb range. Moreover, the altered shape of the pocket results in the modified sensor to no longer sense phenol with high efficiency. In silico docking of the ligand into the $MopR^{IV\_FM\_YF}$ mutant shows that the pocket has undergone several subtle modifications to aptly accommodate 2,3-dmp (Figure 2C and Table S2). Data with each single mutation demonstrates that the pocket architecture gradually (both from affinity as well as biosensing perspective) became conducive towards DmpR design (Figure 2D–G). Results further show that mutation of F132M has the most significant effect in shifting the specificity, as this mutation replaces a rigid aromatic phenyl ring by a flexible long chain hydrocarbon, thereby allowing readjustment and creation of the requisite space for the bulkier ligand (Figures 2D and S3B–D). The triple mutant that mirrors DmpR pocket exhibits the best binding affinity, LOD of 12 ppb and a sensitivity toward 2,3-dmp, which is comparable to the native phenol $MopR^{ABC}$ sensor in the parts per billion range (Figures 2F, 2H and S4). As mentioned earlier, the engineered sensor is primarily a substituted phenol sensor and no longer senses phenol efficiently. These results highlight that recognition of the compound primarily lies in the binding pocket and by implementing evolutionary design on a single soluble protein system, the limitation of coverage of a broad range of pollutant monitoring can be overcome, without compromising biosensing parameters.

Fabrication of the Protein Biosensor Strips. After optimizing the performance of $MopR^{ABC}$ in solution biosensor format, the next step was to convert the enzyme system to a viable strip form. The immobilization process in most cases allow greater portability and storage. This strategy brings the system closer to a translation setup and eventual commercialization. For immobilization of $MopR^{ABC}$, a physical adsorption technique was preferred, as several other enzyme

DOI: 10.1021/acs.analchem.8b01130
Anal. Chem. 2018, 90, 8960–8968

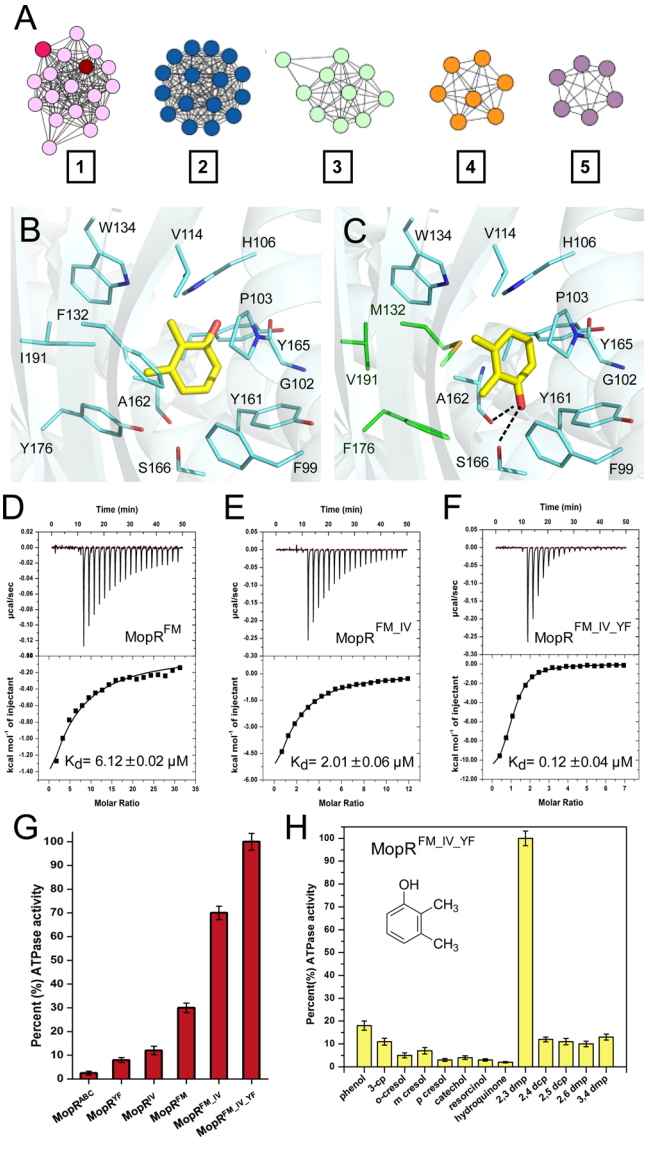

Figure 2. Exclusive 2,3-dimethylphenol sensor design. (A) Cytoscape representation of the sequence similarity network of cog1221 (σ54-based AAA+ ATPases) at an *e*-value cutoff of 10^{-90}. In each group, the nodes represent the proteins and the edges represent the BLASTP linkages. The groups are named based on the characterized protein present in each group (group 1, small molecule sensing regulators; groups 2, cyclic nucleotide binding proteins; group 3, type VI secretion system regulators; group 4, propionate catabolism regulators; group 5 remains unannotated). The proteins under study, MopR (in red) and DmpR (in pink), falls in group 1. (B–C) Docked 2,3-dimethylphenol (2,3-dmp), a representative xylenol, in native and mutated ($MopR^{FM\_IV\_YF}$) MopR construct, respectively. (D–F) ITC of 2,3-dmp with $MopR^{FM}$, $MopR^{FM\_IV}$, and $MopR^{FM\_IV\_YF}$ respectively. (G) ATPase activity in response to 2,3-dmp upon introduction of mutations in the binding pocket. (H) Substrate profile of the $MopR^{FM\_IV\_YF}$ selective design.

biosensor systems inclusive of the commercial glucose sensors have been successfully translated using this approach.[29] Further, it is reported that NtrCs undergo significant conformational changes and oligomerization upon addition of the aromatic sensor molecule.[10] The DLS data corroborates this hypothesis and shows that upon addition of phenol, the population of the $MopR^{ABC}$ protein shifts from a hydrodynamic diameter of 9–16 nm (Figure 3F–G). Hence, physical adsorption was preferred over tethering and other chemical coupling methods, which might hinder conformational flexibility. Because silica nanoparticles are available in various pore diameters and can potentially accommodate protein, either inside the pores or on the surface via adsorption, they were selected as the solid support for creating enzyme-strips (Figure 3A). After trials with a few types of silica nanoparticles, ranging from nonporous to various porous silica, mesoporous silica nanoparticle (MCM-41) with a pore diameter of 6.5 nm yielded the best results (Figure S5A). SEM (scanning electron microscopy) images revealed that the chosen porous silica particles are spherical in nature and arrange spatially across the glass surface on which they were drop-casted (Figure 3B). The high resolution TEM (transmission electron microscopy) images further showed that all MCM-41 samples have well-ordered, parallel arrangement of clearly defined pores, inside each silica particle (Figure 3D). When protein was adsorbed on this support, both SEM and TEM images revealed that at protein concentrations of 2–3 μM, the adsorption was uniform and the protein molecules were wrapped around and in between the mesopores rather than entering into them (Figure 3C, 3E). The honeycomb structure presented by the mesoporous silica allows the slightly larger diameter protein to anchor without compromising its conformational flexibility, such that activity of the sensor was retained, thus making it the most preferred scaffold. Further, BET (Brunauer–Emmett–Teller) data of the silica adsorbed with the protein indicates that $MopR^{ABC}$ is adsorbed on the silica surface rather than going deep inside the mesopores (Figure S5B). A quantitative estimate of the amount of protein immobilized using TGA (thermogravimetric analysis) revealed that 21% weight percentage of $MopR^{ABC}$ protein was loaded onto the silica surface (Figure 3H). Under the above adsorption conditions, enzyme activity and LOD in the strip was at par with solution format (Figure 3I). The engineered sensor strip was also found to be highly sensitive and was capable of detecting a concentration difference of 0.1 μM (10 ppb) in the pollutant sample (Figure 3I). The selectivity of the sensor strip to sense exclusively phenol and smaller phenolics over the bulkier derivatives was also retained with comparable efficiency to the solution format (Figure S6). Further, to ensure that the enzyme strip is a viable option, its shelf life was gauged. Preliminary experiments show that the current design exhibits a stability of 9 days with retention of 50% of the activity (Figure S7). Ongoing efforts to improve the fabrication process are underway. One of the limitations of the MopR system is that all the strips created are one-time use strips. This is because on one hand, the tight binding of phenol although yields high specificity and sensitivity for the system, it results in the enzyme irreversibly binding to phenol and constitutively activating the ATP hydrolysis. Despite this shortcoming, the ease of production of the enzyme, long shelf life, and the relatively simple fabrication process can yield a process with a low production cost per enzyme-strips. Therefore, this system can be envisioned as a viable option for further development and commercialization.

Potential Viability of the Biosensor Strip for Environmental Wastewater Analysis. The next step was to test the viability of the sensor strip in a crowded environment, as regularly encountered in a real time setting. In polluted water bodies, phenol and its derivatives are present along with a mixture of diverse pollutants; hence, selective and direct detection becomes difficult. Therefore, it is envisioned that the

DOI: 10.1021/acs.analchem.8b01130
Anal. Chem. 2018, 90, 8960–8968

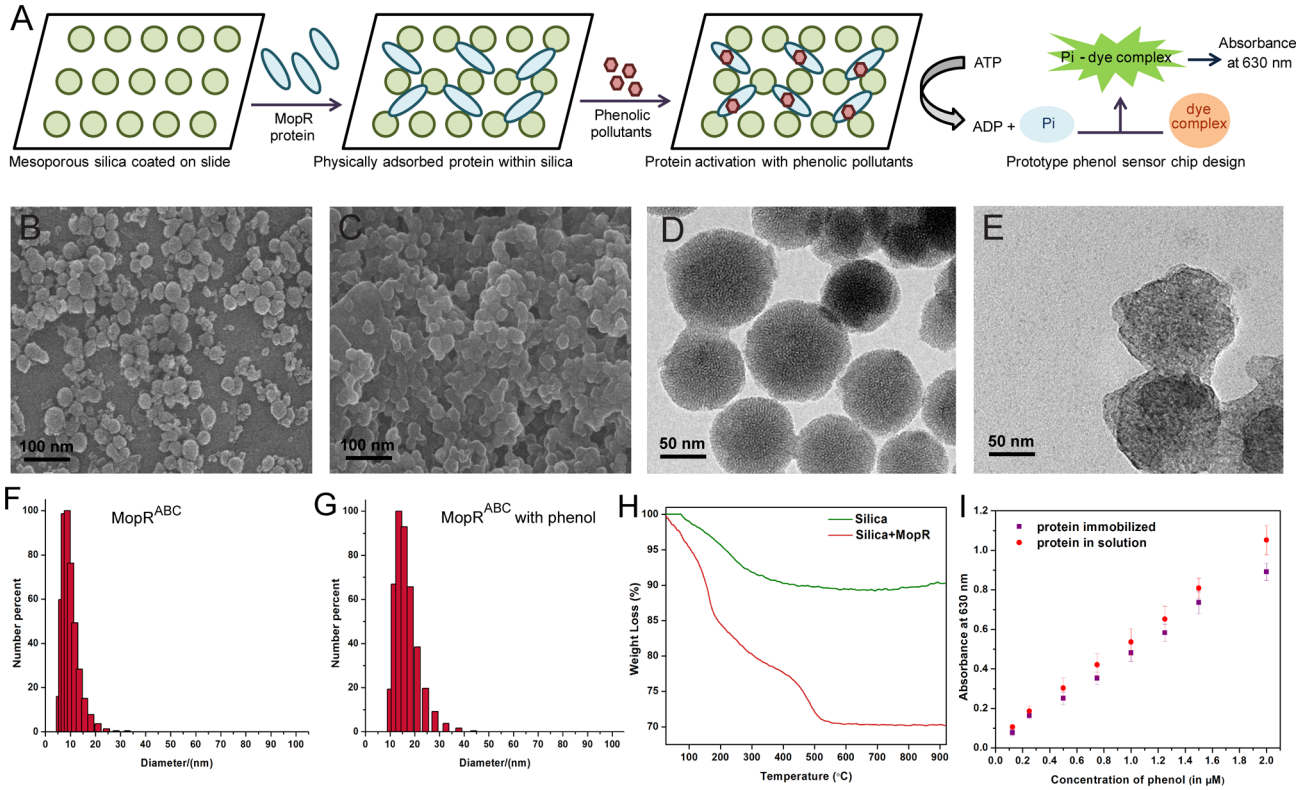

Figure 3. Design and characterization of protein sensor chip. (A) Schematic representation of the MopR^{ABC} protein based biosensor strip design. (B–C) SEM images of MCM-41 (B), MCM-41 with adsorbed protein (C) and (D–E) TEM images of MCM-41 (D), MCM-41 with adsorbed protein (E) showing the external particle morphology of the spherical MCM-41 before and after protein adsorption.

efficient MopR^{ABC} biosensor technology will provide an edge for in situ, direct detection in contaminated environmental samples. To establish this hypothesis, simulated wastewaters (SWW) containing a mix of common pollutants (anionic, cationic, volatile, semivolatile, disinfectants, emerging contaminants) were created. A comparative phenol sensitivity plot (in both standard phenol solutions and SWW) revealed minimal interference (less that 4%) from the other contaminants, even at the lowest detectable phenol concentrations in both solution (Figures 4A and S8), as well as strip format (Figure 4B). A similar selectivity analysis of the MopR^{FM_IV_YF} sensor and its performance in SWW crowded with various pollutants was compared. The results revealed that the engineered sensor is efficient and exclusively senses 2,3-dmp without any loss of sensitivity (Figure S9). These results highlight that the engineered sensor designs can be extended towards testing in real time environmental samples. Therefore, real samples were collected from two different water bodies (Mithi River, EVS1 and Powai Lake, EVS2). The native MopR^{ABC} phenol sensor performance in the strip format was calculated and the phenol content in EVS1 (~65 ppb/0.65 μM), EVS2 (~33 ppb/0.33 μM) and local tap water sample (~12 ppb/0.12 μM) were ascertained (Figure 4C–D). The fidelity of the sensor in strip format was maintained for multiple samples and comparable results in both solution as well as strip format (with less than 5% error) indicates excellent translation potential of the immobilized strip design. To further verify the accuracy of the sensor design, independent chemical analysis of EVS1, EVS2, and tapwater was also performed using standard protocols (described in details in Experimental Section).[30] The results were in coherence with our biosensor data (Figure 4D). A 10% increment was observed which is attributed to the fact that the chemical analysis estimates overall phenolic content. The latter includes all compounds having the phenolic OH group, while the MopR^{ABC} biosensor specifically only detects phenol and few smaller phenol derivatives. Hence, these observations clearly indicate that the MopR^{ABC} biosensor has a strong potential for future creation of a prototype device. The ability of this system toward direct detection of low phenol content in the 10 ppb/0.1 μM range extends the utility of this sensor for potential instant, direct detection in drinking water, down to the common household levels.

CONCLUSION

The MopR^{ABC} based phenol biosensor reported in this work displays a novel and robust enzyme system, possessing several promising qualities towards a translational potential. The enzyme system is thermostable, a quality that is difficult to achieve in biological sensors. Moreover, the system is versatile and not only offers selectivity and sensitivity but also has the unique ability to be tunable, facilitating design of a repertoire of biosensors. Consequently, MopR^{ABC} design can be extended to encompass sensing of a spectrum of aromatic pollutants, where specific and accurate determination of each pollutant type can be achieved and remediation techniques for the individual pollutant can be appropriately implemented. The added benefit that this system presents is that it is malleable and translation into a strip-based format is possible. The ease of translation into an immobilized strip format, without any loss of enzyme efficiency, makes it a very promising candidate for prototype device fabrication, for direct detection of aromatic pollutants from real time environmental samples. Attempts are further ongoing in the laboratory to improve the

DOI: 10.1021/acs.analchem.8b01130
Anal. Chem. 2018, 90, 8960–8968

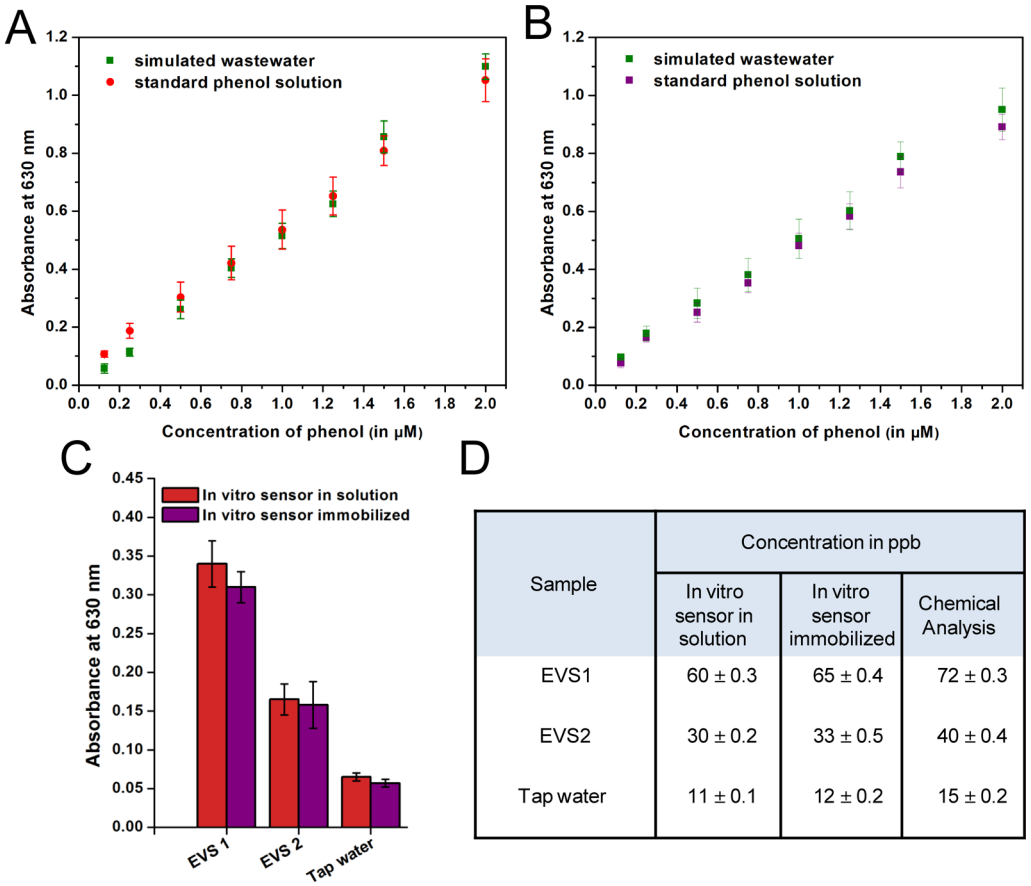

Sample	Concentration in ppb		
	In vitro sensor in solution	In vitro sensor immobilized	Chemical Analysis
EVS1	60 ± 0.3	65 ± 0.4	72 ± 0.3
EVS2	30 ± 0.2	33 ± 0.5	40 ± 0.4
Tap water	11 ± 0.1	12 ± 0.2	15 ± 0.2

Figure 4. Commercial viability of sensor strip design. (A, B) Comparative biosensing efficiency and sensitivity of the sensor design in solution (A) and strip format (B) with standard phenol solution and SWW. Phenol detection is retained with 97% efficiency. (C) Testing of environmental samples (tap water and EVS1, EVS2 which are contaminated waters) in solution as well as immobilized form. (D) Total phenol content (in ppb) represented as mean ± standard deviation of three triplicate readings. The amount of phenol in each sample was calculated based on the slope of the standard phenol sensitivity plot. The overall pollutant concentrations were found to be 90% accurate when compared to a standard chemical analysis of total phenolic content in the samples.

shelf life of the biosensor strip design and convert it into a portable device format for in situ pollutant monitoring.

EXPERIMENTAL SECTION

DNA Manipulations, Overexpression, and Purification of the Recombinant Proteins. The purified genomic DNA of *Acinetobacter calcoaceticus* NCIB8250 (2ug/μL) was used as a template for the PCR amplification of the signal-sensing (A) and ATPase (C) domain of native MopR (MopR^{ABC}) gene. The amplified MopR^{ABC} gene was cloned into a modified pET expression vector, which adds a His tag to the protein. The recombinant construct of native MopR^{ABC} was used as a template to make the following binding pocket mutations: MopR^{IV} (valine substitution of I191), MopR^{FM} (methionine substitution of F132), MopR^{YF} (phenylalanine substitution of Y176), and their corresponding double (MopR^{FM_IV}) and triple (MopR^{FM_IV_YF}) mutants. All the point mutations were performed employing standard site-directed mutagenesis protocol using the "site-directed mutagenesis kit" from Kapa biosystems. The native and mutant protein constructs were subsequently transformed into *Escherichia coli* BL2(DE3)plysS cells and grown at 37 °C until OD_{600} reached 0.6−0.8 and then induced with 0.7 mM IPTG (isopropyl-β-D-thiogalactopyranoside) at 16 °C. All these protein constructs were purified using Ni-NTA resin employing standard His-tagged affinity purification protocol as described previously.[16] The eluted fractions were further concentrated and desalted with buffer containing 25 mM Tris buffer, pH 7.5; 100 mM NaCl using an Econo- Pac 10DG (Bio-Rad, CA, USA) column. All the desalted fractions were pooled together, concentrated up to 6−8 mg/mL, flash-frozen in liquid N_2, and stored at −80 °C until they were used.

CD-Based Thermal Shift assay. A host of truncated versions of the native MopR^{ABC} protein (consisting of residues in the range of 470−510 amino acids) were cloned and purified using the protocol described above. The proteins were screened and the soluble constructs were identified (construct 1 and 2) which were then tested using CD-based thermal denaturation experiment to ascertain the optimal thermostable construct which would be used as the biosensing template. Scans were performed at a temperature range of 20 to 95 °C using 0.1 cm path length quartz cuvettes with 16 s differential integration time at a scan rate of 100 nm/s with 3 min delay time per temperature change.

In Vitro ATPase Assay Design. To perform the in vitro biosensing ATPase assay, 2 μM of protein sample (native and mutated MopR^{ABC}) was first incubated with varying concentrations (0.1, 1, 10, 100, 1000 μM) of each aromatic compounds to be tested. On the basis of the pollutant response profile (Figures 1, 2, S2, and S4), pollutants in the range of 0.1−10 μM were used in further studies, which lie

DOI: 10.1021/acs.analchem.8b01130
Anal. Chem. 2018, 90, 8960−8968

within the approximate environmental risk limits for these pollutants as per Occupational Safety and Health Administration (OSHA). The ATPase assay was performed based on protocol reported previously.[16] For the time-dependent activity assay, 2 μM of the native MopR^{ABC} protein, stored over a time-period of 20 days, was tested for ATPase activity (on incubation with 10 μM of phenol) every fifth day. For the temperature-dependent activity assay, 2 μM of the native protein was heated to a particular temperature (25−90 °C) and tested for ATPase activity (on incubation with 10 μM of phenol). Each of the experiments was performed in triplicates and the standard error estimate has been represented as error bars within the figures.

Sequence Similarity Network. To generate a sequence similarity network, protein sequences belonging to cog1221 were retrieved from NCBI database in FASTA format. An all-by-all BLAST with an e value cutoff of 10^{-90} was performed using BLAST+ and BLAST2 sim plugin software from the NCBI site. This generated a BLAST on BLAST file for each pair, and the output was loaded into Cytoscape to visualize the network as evolutionarily distinct groups.[28]

Docking Studies. On the basis of the detailed analysis of the pollutant binding pocket using the phenol bound crystal structure of the signal sensing domain of MopR (MopR^{AB}) (Figure S2A), the same site-specific mutations of the pocket residues as described above were designed in silico to accommodate the bulkier phenol derivatives. Docking experiments of all these mutants were performed with phenol and 2,3-dimethylphenol (2,3-dmp) to test whether the modified pocket of MopR could accommodate 2,3-dmp with favorable binding energetics. A monomeric subunit of the X-ray structure of the MopR-effector complex (PDB code 5KBE)[15] was used for docking so as to predict affinity of the MopR mutants toward different pollutants. The template PDB used for the docking experiments was manually modified each time based on the mutants used. The final MopR mutant PDBs used for docking had the previously present ligand coordinates deleted from them. All docking runs were conducted by using a genetic algorithm (GA) in AutoDock version 4.2 against the target aromatic effectors.[31] Each ligand for a particular mutant version of MopR was scored according to a free energy cost function (ΔG^*) that accounts for van der Waals, hydrogen bonding, electrostatic, solvation, and torsional free energy terms. The grid box for docking was selected in the binding pocket region, and rigid docking was performed with 250 runs for each ligand−MopR^{AB} mutant combinations. On the basis of the estimated free energy of binding (ΔG^*) calculated in docking, the top-ranked ligand orientations were selected (listed in Table S2).

ITC Experiments. To validate the docking results, ITC (Isothermal Calorimetry) experiments were performed using MicroCal iTC200 (GE Healthcare). All the protein (native and mutated MopR^{ABC}) and ligand samples (phenol and 2,3-dmp) were prepared in a buffer that contained 25 mM HEPES (pH-7.5) and 80 mM NaCl (buffer A). In the ITC experiments, all the aromatic effectors were titrated against buffer A and subtracted from the raw data prior to model fitting to nullify the heat of dilution. The sample cell that contained 10−50 μM protein was titrated with 100−700 μM of the effectors. The concentrations of protein and ligand used in different ITC experiments varied as per requirement to attain optimal saturation for a particular titration curve. The volume of the titrant (effector) added at each injection into the sample cell was 2 μL for 5 s. A range of 20−40 injections was performed for each experiment with an interval of 120 s between each successive injection. The temperature was maintained at 25 °C. The stirring rate was kept constant at 1000 rpm throughout the ITC experiments. The data obtained were fitted and analyzed using one set of sites model with Origin 7 software. All ITC experiments were conducted three times and then averaged to determine the final values.

Preparation of Mesoporous Silica. For physical adsorption of MopR^{ABC} protein, mesoporous silica nanoparticles (MCM-41) were used, which were functionalized using the following protocol. Initially, 0.25 g of CTAB (surfactant) was added in 120 mL of deionized water, followed by addition of 0.875 mL of 2 M NaOH to it. The resulting solution was stirred for 1 h at 300 rpm and 35 °C. Decane (0.6 mL, expander) was then added and the solution was further stirred for 4 h at 35 °C. Temperature was then raised to 80 °C and 1.25 mL of TEOS, (MCM-41 silica precursor) was added to the solution. Stirring was further continued for 30 min at 80 °C. After that the solution was cooled down to room temperature. The silica nanoparticles were then collected by centrifugation at 14 000 rpm for 10 min. Solid products were filtered and washed several times using water. It was dried overnight in oven. Later, to remove the surfactant CTAB by calcination, the nanoparticles were heated in furnace at 540 °C for 6 h. The MCM-41 mesoporous silica were stored at room temperature prior to further use.

Physical Adsorption of MopR in Silica. Twenty milligrams of mesoporous silica was dissolved in 1 mL of water and sonicated for 30 min to make a uniform suspension. The silica suspension was evenly coated on glass coverslips (3 × 3 mm) by dropcasting and dried for around 2 h. Optimized amount of protein-buffer solution (pH 8.5) was dispersed next onto silica surface and kept for drying, for about 90 min for optimal physical adsorption. The adsorbed protein (MopR^{ABC}) on silica was further characterized by various analytical techniques like SEM, TEM, BET, TGA, etc., as detailed below and was finally used as a prototype biosensor strip for performing the in vitro biosensing assay.

Scanning Electron Microscopy (SEM). The SEM imaging of the MCM-41 silica with and without the adsorbed MopR^{ABC} protein was done on an Hitachi SEM-OIM (Fei Quanta 200 HV SEM with TSL-EDX) under an accelerating voltage of 10−15 kV.

Transmission Electron Microscopy (TEM). A Philips CM 200 transmission electron microscope, operating under an accelerating voltage of 200 kV, was used for imaging of MCM-41 silica nanoparticles with and without MopR^{ABC} protein. Protein and silica samples were prepared by mixing equal volumes of both protein and silica solution and then loading a drop of the mixture onto Formvar-coated 300 mesh copper grid, which was further air-dried before collecting the images.

Brunauer−Emmett−Teller (BET) Analysis. Nitrogen sorption measurements were conducted at liquid nitrogen temperature (77 K) using a Quantachrome Autosorb adsorption analyzer. Samples were degassed at 150 °C for 6 h. Pore diameters were estimated from adsorption branch of the isotherm, using the BJH model. Surface areas were calculated using the BET model in the relative pressure range of 0.05−0.3. Total pore volumes were estimated at a relative pressure of 0.995, assuming full surface saturation of nitrogen.

Thermogravimetric Analysis (TGA). Thermogravimetric analysis (TGA) was performed on Shimadzu DT-30 Thermal

DOI: 10.1021/acs.analchem.8b01130
Anal. Chem. 2018, 90, 8960−8968

Analyzer instrument, by heating the samples (silica and silica with protein) up to 1000 °C, at a constant rate of 10 °C min^{-1}, under an N_2 atmosphere.

Dynamic Light Scattering (DLS). A ZEN 1600 (red) Particle Size Analyzer from Malvern Instruments, was used for determination of the size distribution of the $MopR^{ABC}$ protein, at 298 K and pH 8.5. The instrument laser operates at 632.8 nm.

Activity Assay and Shelf Life of the Immobilized Protein Strips. The immobilized $MopR^{ABC}$ protein strips were tested for enzyme activity, selectivity, and sensitivity toward phenol sensing, both by using the same in vitro colorimetric Malachite green based ATPase assay, with exactly identical assay parameters as optimized for the protein in solution. For the shelf life analysis, a series of $MopR^{ABC}$ protein strips were prepared and stored at 4 °C and each day (up to a period of 10 days), a strip was taken out and its activity and phenol sensing efficiency was tested using the established ATPase assay protocol.

Interference Assay with Simulated Wastewater (SWW) Sample. For performing the pollutant interference assay, simulated wastewater (SWW) sample (mimicking a real time contaminated environmental sample) was first prepared by mixing together different commonly found environmental pollutants (at 1 mM concentration of each). They include benzene as representative semivolatile organic contaminant, acetone and ethyl acetate as representative volatile organic contaminants, NH_4^+ and Sr^{2+} as representative cationic contaminants, Cl^- and F^- as representative anionic contaminants, Co^{2+} and Zn^{2+} as representative metal contaminants, Hg^{2+}, styrene, ampicillin, and tylosin as representative emerging contaminants, and perchlorate as representative disinfection byproduct contaminant. Native $MopR^{ABC}$ (2 μM), which can preferentially sense only phenol in a milieu of environmental contaminants, and $MopR^{FM\_IV\_YF}$, which preferentially senses 2,3-dimethylphenol in a mix of environmental contaminants, were incubated with different concentrations of phenol (0.1−2 μM) and 2,3-dmp(0.1−2 μM) respectively in SWW and tested for interference from other pollutants. The in vitro ATPase assay protocol, as described above was used to gauge specificity. The resultant ATPase activities obtained were compared with the standard activity of native $MopR^{ABC}$ and $MopR^{FM\_IV\_YF}$, in response to similar concentrations of standard phenol and 2,3-dmp solutions, respectively. A similar set of interference tests were performed with the native $MopR^{ABC}$ biosensor strips. All the absorbance values have been represented as percent ATPase activity. Each of the experiments was performed in triplicates and the error estimate has been represented as error bars within the figures.

Environmental Sample Testing. Wastewater samples were procured from two contaminated water bodies namely Mithi river (EVS1) and Powai lake (EVS2) from across the city of Mumbai, India. Tap water samples were collected from faucets inside IIT Bombay. To remove any particulate matter, all the samples were filtered using 0.2 μm filters and calibrated at pH 7.0, prior to testing. By employing the in vitro native $MopR^{ABC}$ phenol sensor in both solution and strip (immobilized) format, all the environmental samples were tested directly without any other pretreatment steps and the phenol content measured. The total concentration of phenol in each sample was determined by the in vitro sensor, with the relevant standard sensitivity curve.

Chemical Analysis of Phenolic Compounds. To confirm the data obtained from our biosensing assay, chemical analysis of the environmental wastewaters (filtered and pH adjusted) were performed, according to the standard methods recommended by EPA (Environmental Protection Agency, USA).[30] Each sample of wastewater was treated with 25 μL of 0.5N NH_4OH, 10 μL of 2% 4-aminoantipyrine (Sigma, MO), and 10 μL of 8% $K_3Fe(CN)_6$ (Sigma, MO) in a sequential manner, in a 1 mL sample volume, and then mixed thoroughly and measured at OD_{500} nm. The total phenolic content (concentration of all pollutants having the phenolic OH group) in each sample was precisely determined using standard concentration curve as obtained using the same analysis.

■ ASSOCIATED CONTENT

Supporting Information

The Supporting Information is available free of charge on the ACS Publications website at DOI: 10.1021/acs.analchem.8b01130.

Stability and activity analysis of $MopR^{ABC}$, substrate scope and sensitivity of native $MopR^{ABC}$ sensor, structural guided tuning of $MopR^{ABC}$ pocket, substrate scope and sensitivity of $MopR^{FM\_IV\_YF}$ sensor, optimization of the $MopR^{ABC}$ strip design, selectivity analysis of native $MopR^{ABC}$ sensor in strip format, shelf-life of the $MopR^{ABC}$ sensor strip design, ATPase activity of native $MopR^{ABC}$ sensor, interference assay of $MopR^{FM\_IV\_YF}$ biosensor, list of phenol-sensing protein-based biosensors, and docking of MopR mutants with different aromatic pollutants (PDF)

■ AUTHOR INFORMATION

Corresponding Author

*E-mail: ruchi@chem.iitb.ac.in.

ORCID

Rajdip Bandyopadhyaya: 0000-0001-5902-5171

Ruchi Anand: 0000-0002-2045-3758

Author Contributions

R.A., S.R., and R.B. designed research; S.R., T.M., and S.S. performed research; R.A. and R.B. contributed new reagents/analytic tools; S.R., T.M., S.S., R.A., and R.B. analyzed data, and R.A. and S.R. wrote the paper.

Notes

The authors declare no competing financial interest.

■ ACKNOWLEDGMENTS

We thank the members of Colloids and Nanomaterials group, Chemical Engineering Department, IIT Bombay, for providing the various silica nanoparticles. We also thank the Sophisticated Analytical Instrument Facility (SAIF), Central Facility of Chemistry and Chemical Engineering Department at IIT Bombay for access to instrumentation. This work was funded by DST, Government of India (Grant Numbers EMR/2015/002121 and DST/TM/WTI/2K16/252) .

■ REFERENCES

(1) Mehrotra, P. *J. Oral Biol. Craniofac. Res.* **2016**, *6* (2), 153−159.
(2) Lin, Y.; Lu, F.; Tu, Y.; Ren, Z. *Nano Lett.* **2004**, *4* (2), 191−195.
(3) Wilson, R.; Turner, A. P. F. *Biosens. Bioelectron.* **1992**, *7* (3), 165−185.
(4) Fortier, G.; Brassard, E.; Bélanger, D. *Biosens. Bioelectron.* **1990**, *5* (6), 473−490.

DOI: 10.1021/acs.analchem.8b01130
Anal. Chem. 2018, 90, 8960−8968

(5) Van Emon, J. M.; Lopez-Avila, V. *Anal. Chem.* **1992**, *64* (2), 78A−88A.
(6) Daniels, J. S.; Pourmand, N. *Electroanalysis* **2007**, *19* (12), 1239−1257.
(7) Vollmer, F.; Arnold, S. *Nat. Methods* **2008**, *5* (7), 591.
(8) Galvão, T. C.; De Lorenzo, V. *Curr. Opin. Biotechnol.* **2006**, *17* (1), 34−42.
(9) Timmis, K. N.; Pieper, D. H. *Trends Biotechnol.* **1999**, *17* (5), 201−204.
(10) Bush, M.; Dixon, R. *Microbiol. Mol. Biol. Rev.* **2012**, *76* (3), 497−529.
(11) Shingler, V. *Mol. Microbiol.* **1996**, *19* (3), 409−416.
(12) Tropel, D.; van der Meer, J. R. *Microbiol. Mol. Biol. Rev.* **2004**, *68* (3), 474−500 table of contents.
(13) Morett, E.; Segovia, L. *J. Bacteriol.* **1993**, *175* (19), 6067−6074.
(14) Schirmer, F.; Ehrt, S.; Hillen, W. *J. Bacteriol.* **1997**, *179* (4), 1329−1336.
(15) Ray, S.; Gunzburg, M. J.; Wilce, M.; Panjikar, S.; Anand, R. *ACS Chem. Biol.* **2016**, *11* (8), 2357−2365.
(16) Ray, S.; Panjikar, S.; Anand, R. *ACS Sens.* **2017**, *2* (3), 411−418.
(17) Wille, K.; De Brabander, H. F.; Vanhaecke, L.; De Wulf, E.; Van Caeter, P.; Janssen, C. R. *TrAC, Trends Anal. Chem.* **2012**, *35*, 87−108.
(18) Park, M.; Tsai, S.-L.; Chen, W. *Sensors* **2013**, *13* (5), 5777.
(19) Ozoner, S. K.; Erhan, E.; Yilmaz, F. Enzyme based phenol biosensors. *Environmental Biosensors*; Somerset, V., Ed.; InTech, 2011.
(20) Rodríguez-Delgado, M. M.; Alemán-Nava, G. S.; Rodríguez-Delgado, J. M.; Dieck-Assad, G.; Martínez-Chapa, S. O.; Barceló, D.; Parra, R. *TrAC, Trends Anal. Chem.* **2015**, *74*, 21−45.
(21) Campuzano, S.; Serra, B.; Pedrero, M. a.; de Villena, F. J. M.; Pingarrón, J. M. *Anal. Chim. Acta* **2003**, *494* (1-2), 187−197.
(22) Korkut, S.; Keskinler, B.; Erhan, E. *Talanta* **2008**, *76* (5), 1147−1152.
(23) Geladopoulos, T. P.; Sotiroudis, T. G.; Evangelopoulos, A. E. *Anal. Biochem.* **1991**, *192* (1), 112−116.
(24) Hildén, K.; Hakala, T. K.; Lundell, T. *Biotechnol. Lett.* **2009**, *31* (8), 1117.
(25) Pravda, M.; Petit, C.; Michotte, Y.; Kauffmann, J.-M.; Vytřas, K. *J. Chromatogr. A* **1996**, *727* (1), 47−54.
(26) Chang, T.-S. *Int. J. Mol. Sci.* **2009**, *10* (6), 2440−2475.
(27) Brijwani, K.; Rigdon, A.; Vadlani, P. V. *Enzyme Res.* **2010**, *2010*, 149748.
(28) Atkinson, H. J.; Morris, J. H.; Ferrin, T. E.; Babbitt, P. C. *PLoS One* **2009**, *4* (2), No. e4345.
(29) Ram, M. K.; Adami, M.; Paddeu, S.; Nicolini, C. *Nanotechnology* **2000**, *11* (2), 112.
(30) Shin, H. J.; Park, H. H.; Lim, W. K. *J. Biotechnol.* **2005**, *119* (1), 36−43.
(31) Morris, G. M.; Huey, R.; Lindstrom, W.; Sanner, M. F.; Belew, R. K.; Goodsell, D. S.; Olson, A. J. *J. Comput. Chem.* **2009**, *30* (16), 2785−91.

DOI: 10.1021/acs.analchem.8b01130
Anal. Chem. 2018, 90, 8960−8968